Monte Carlo Calculations on Electron Backscattering in Amorphous or Polycrystalline Targets

G. Soum
Laboratoire associé à l'Université Paul Sabatier

H. Ahmed
Laboratoire associé à l'Université Paul Sabatier

F. Arnal
Laboratoire associé à l'Université Paul Sabatier

B. Jouffrey
Laboratoire associé à l'Université Paul Sabatier

P. Verdier
Laboratoire associé à l'Université Paul Sabatier

Recommended Citation

Utah State University
MERRILL-CAZIER LIBRARY

MONTE CARLO CALCULATIONS ON ELECTRON BACKSCATTERING IN AMORPHOUS OR POLYCRYSTALLINE TARGETS

G. Soum, H. Ahmed, F. Arnal, B. Jouffrey & P. Verdier

Laboratoire d'Optique Electronique du C.N.R.S.
Laboratoire associé à l'Université Paul Sabatier
B.P. 4347 — 31055 Toulouse Cedex — France
Phone number: (61) 52 65 96

ABSTRACT

We propose an application of the Monte Carlo method in the field of backscattering. The results obtained for incident electron energies ranging from 0.3 to 3 MeV and for targets of Al, Cu, Ag and Au are compared with experimental values from several sources.

An electron travelling through matter undergoes successive collisions between which it is assumed to travel in a straight line. In our case, we consider the elementary process of inter-action electron-nucleus; we have used analytical models for the scattering cross-sections. In order to follow the electron through the specimen, we divide the real trajectory into elements of length much smaller than the mean free path. Pseudo-random number process permits us to determine whether or not an interaction occurs, also the type of inter-action. For the energy losses, we introduced a relation de-rived from Landau's theory. We then followed the electron until it is emerged from the material or halted.

The backscattering coefficients obtained for thin and thick targets as a function of the incident electron energy are in good agreement with the experimental data. We have intro-duced the depth distribution function of the backscattered electrons, which allows us to test the predictions of various theoretical models proposed by other authors.

1. INTRODUCTION

The backscattering of high energy electrons from solids has become a subject of ever-increasing interest in recent years, especially because of its applications in microanalysis and scanning electron microscopy. We are interested in the backscattering of electrons by polycrystalline targets of aluminium, copper, silver and gold, for normal incidence and for energies ranging from 0.3 to 3 MeV.

In principle, the solution of the Boltzman transport equa-tion allows us to determine the trajectory of electrons in mat-ter; the first important works are those of Bethe et al. (1938). The correct analytical solution of this equation is difficult to obtain, although several different methods have been pro-posed (Brown et al. 1969). All past treatments do not give an analytical solution of this equation (Bennett and Roth, 1972; Brown and Ogilvie, 1966; Fathers and Rez, 1979; Lanteri et al. 1980).

Some years ago, the numerical procedures known as Monte Carlo methods were developed (Berger, 1963; Bishop, 1967; Henoc, 1976; Martinez and Balladore, 1979). The problem is solved statistically. Monte Carlo methods are more suitable than those using Boltzman's equation; they also have many advantages over the various theories of mul-tiple scattering. Furthermore, we need not introduce the small angle approximation in order to perform the calcula-tion; as the electron passes through an element, we consider the broadening of the electron beam and we take the energy loss and the inelastic scattering into account.

We explain our application of the Monte Carlo method to the phenomenon of backscattering and we use a theoretical model for the cross section and energy losses. For the ele-ments studied, we give the value and magnitude of the phy-sical variables investigated: backscattering coefficient, angular energy and depth distributions of backscattered elec-trons. For each case, we compare the results given by our cal-culation with the experimental results given by different authors or by different theoretical published models.

2. METHOD OF CALCULATION

2.1 Generalities

We simulate the trajectory of each electron by generation of uniform pseudo-random numbers X, which must be un-correlated and distributed uniformly between zero and one.

G. Soum, H. Ahmed, F. Arnal, B. Jouffrey & P. Verdier

LIST OF SYMBOLS

X	=	Pseudo-random number
x	=	Specimen thickness
Q	=	Differential scattering cross section per unit solid angle
σ	=	Total scattering cross section
e,i	=	Subscripts respectively elastic, inelastic
Z	=	Atomic number
β	=	Ratio of electron velocity to light velocity
m	=	Electron mass
e	=	Electron charge
$h = \hbar.2\pi$	=	Planck's constant
$\vec{k}$	=	Wave vector
Θ_0	=	Screening angle
N_a	=	Avogadro's number
α	=	Half-aperture angle
Δs	=	Path-length element
Λ	=	Mean free path
ϱ	=	Density of target material
A	=	Atomic mass
E_0	=	Kinetic energy of the electron beam
ΔE	=	Energy loss
ΔE_m	=	Mean energy loss
ΔE_p	=	Most probable energy loss
$r(E_0)$	=	Total electron range
R	=	Backscattering coefficient

For each number X and after the electron has travelled a path length in the element equal to Δs, we associated an angular deviation Θ such that

$$X = 2\pi \int_0^\theta F(\chi) \sin \chi \, d\chi \qquad 1$$

The angular distribution $F(\chi)$ during each step Δs must be known; we find in the literature two different methods for executing Monte Carlo calculations:

• If the path length element Δs is so short that we can consider that only one event will take place, then $F(\chi)$ is directly connected with the differential cross section; this is the single-scattering model (Matsukawa et al. 1973; Murata, 1974; Reimer et al. 1970, Soum et al. 1979, 1981a);

• If, on the contrary, several events take place during the path length element Δs, we choose a multiple scattering law for $F(\chi)$ (Bishop, 1967; Shimizu and Murata, 1971).

In both cases, we must compute the step path length between successive events and any energy loss suffered by the electron. We have chosen the single scattering model. We use the direct sample method for the distribution of path length and we take Landau's theory for the energy loss-law rather than that of Bethe. This law has been investigated experimentally in the energy range studied here (Perez et al. 1977).

2.2 Angular deviation

2.2.1 Principle As we are considering elementary processes, the differential cross section for an event gives the angular distribution after that event directly. The distribution function has to satisfy the normalization condition and, thus, we have:

$$F(\chi) = \frac{1}{\sigma} Q(\chi) \qquad \text{with } \sigma = \int_0^\pi Q(\chi) \, 2\pi \sin \chi \, d\chi.$$

The deviation angle Θ of the electron from the initial direction is obtained by generating a random number X, according to Equation 1. Because of the spherical symmetry of the isolated atoms, the azimuth Φ of the trajectory becomes a simple second number $\Phi = 2\pi X$.

Knowing the deviation (Θ, Φ) resulting from the interaction, we determine the direction cosines of the trajectory. It is then possible to express the electron angular characteristics at the beginning of each step in terms of the parameters of the preceding step.

2.2.2 Elastic scattering In high energy electron microscopy, the first Born approximation is found justified; this is expressed by the relation $\alpha' \ll 1$ with $\alpha' = Z/137\beta$. When we consider Wentzel's potential, which has only one exponential term, in the first Born approximation, we obtain (Arnal et al. 1977):

$$Q_e(\chi) = \frac{Z^2 m^2 e^4}{4(\hbar k)^4 (1 - \beta^2)} C^2 \frac{1}{(\sin^2 \frac{\chi}{2} + \frac{\Theta_0^2}{4})^2} \qquad 2$$

$C = \exp(b/a)$ is a characteristic parameter of the target atoms. The coefficients a and b are written respectively:

$$a = (32.4 + 0.213 Z)Z^{-1/3}$$
$$b = \exp\{2(1 - 0.0157 Z)\}$$

Thus, the elastic mean free path is given by:

$$\frac{1}{\Lambda_e} = \frac{\varrho N_a}{A} \frac{4\pi Z^2 m^2 e^4}{(\hbar k)^4 (1 - \beta^2)} C^2 \frac{1}{\Theta_0^2} \qquad 3$$

After integration and inversion of Eq. 2, we determine the scattering angle Θ for an elastic collision:

$$\cos \Theta = 1 - \frac{\Theta_0^2}{2} \frac{X}{1 - X + (\frac{\Theta_0}{2})^2} \qquad 4$$

2.2.3 Inelastic scattering In order to simulate the process of the inelastic scattering, we must separate the valence electrons from those which are lightly bound to the nucleus. We have studied the domain of plural and multiple scattering (Soum et al. 1979). We can neglect plasmon scattering which is highly concentrated within small angles. In Morse's approximation and for Wentzel's potential, we obtain (Arnal et al. 1977):

$$Q_i(\chi) = \frac{4 Z m^2 e^4}{(\hbar k)^4 (1 - \beta^2)} C \frac{(\chi^2 + \Theta_E^2)(2 - C) + 2\Theta_0^2}{(\Theta^2 + \Theta_E^2)(\Theta^2 + \Theta_E^2 + \Theta_0^2)^2} \qquad 5$$

where $\Theta_E = \gamma \Delta E / (\gamma^2 - 1)mc^2$ is the minimum scattering

angle, corresponding to the minimum transfer of momentum. For ΔE, we use Berger and Seltzer's (1964) formula:

$$\Delta E = 9.76\,Z + 58.5\,Z^{-0.19} \qquad 6$$

Thus, in the case of an inelastic collision, Eq. 1 tends to:

$$X = \{2\,\text{Log}\,(\frac{\Theta_0}{\Theta_E})^2 + 2\,\text{Ln}\,\frac{\Theta^2}{\Theta^2 + \Theta_0^2} - C\,\frac{\Theta^2}{\Theta_0^2 + \Theta^2}\}$$

$$\{2\,\text{Ln}\,(\frac{\Theta_0}{\Theta_E})^2 - C\}^{-1} \qquad 7$$

Numerical solution of this equation by successive approximations gives us the inelastic scattering angle.

2.2.4 Multiple scattering range In order to save computing time, the angular deflection is determined from the expression for the partial scattering cross section, which is given for elastic scattering outside an angle α by:

$$\sigma_e(\alpha) = \int_\alpha^\pi Q_e(\chi)\,d\Omega = \frac{\pi\,Z^2\,m^2\,e^4}{(\hbar k)^4\,(1-\beta^2)}\,C^2$$

$$\frac{1}{(\sin^2\frac{\alpha}{2} + \frac{\Theta_0^2}{4})} \qquad 8a$$

We have used the calculation of Lenz (1954) in Morse's approximation. The partial inelastic scattering cross section outside an angle α is given by the following expression:

$$\sigma_i(\alpha) = \int_\alpha^\pi Q_i(\chi)\,d\Omega = \frac{4\pi\,Z\,m^2\,e^4}{(\hbar k)^4\,(1-\beta^2)}\,\frac{C^2}{\Theta_0^2}$$

$$\{\frac{2}{C}\,\text{Ln}(1 + \frac{\Theta_0^2}{\alpha^2 + \Theta_E^2})$$

$$-\frac{1}{1 + (\frac{\alpha^2 + \Theta_E^2}{\Theta_0^2})}\} \qquad 8b$$

In Fig. 1, we compare our experimental results (Arnal et al. 1977) and those of Martinez (1978) with the values of $\sigma(\alpha) = \sigma_e(\alpha) + \sigma_i(\alpha)$ given by the above relation. Good agreement of the proposed model with the measurements is found, and Eq. 8 has therefore been chosen for the Monte Carlo calculation.

The scattering outside an angle α with $\alpha \gg \Theta_E$ avoids the difficulties encountered in calculating the inelastic cross section caused by the determination of Θ_E. For elastic scattering outside an angle α, we then obtain:

$$\frac{1}{\Lambda_{e\alpha}} = \frac{\varrho N_a}{A}\,\frac{4\pi\,Z^2\,m^2\,e^4}{(\hbar k)^4\,(1-\beta^2)}\,C^2\,\frac{1}{\Theta_0^2 + \alpha^2} \qquad 9$$
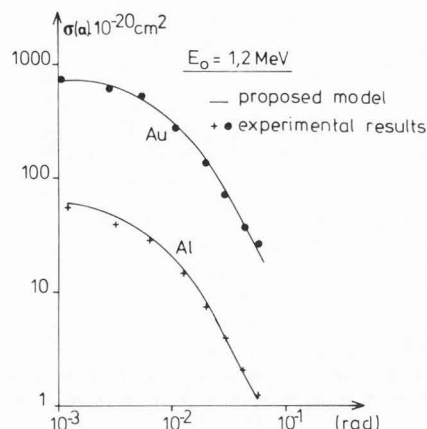

Fig. 1. Variation of scattering cross section outside α.

Table 1. Silver-mean free path (in μm)

V (kV)	Λ_e		$\Lambda_{e\alpha}$ (1); $\Lambda_{i\alpha}$ (2); Λ_α (3) α (rad)		
			0.03	**0.045**	**0.056**
		(1)	0.0825	0.136	0.190
300	0.039	(2)	3.149	6.827	10.60
		(3)	0.0804	0.134	0.186
		(1)	0.254	0.503	0.749
750	0.0544	(2)	14.105	32.203	50.20
		(3)	0.249	0.495	0.738
		(1)	0.496	1.04	1.58
1200	0.059	(2)	31.03	71.11	113.78
		(3)	0.488	1.026	1.558

$$\cos\Theta = \frac{1 - X\Theta_0^2/2(1 - \sin^2\alpha/2) + \sin^2(\alpha/2)(\Theta_0^2/2 + 2)}{(\Theta_0/2)^2 + 1 - X + X\sin^2\alpha/2} \qquad 10$$

where $\Lambda_{e\alpha}$ represents the elastic mean free path for which an electron is scattered with an angle greater than α; similarly, we characterize the inelastic scattering outside an angle α by the expressions:

$$\frac{1}{\Lambda_{i\alpha}} = \frac{1}{Z\Lambda_e}\,\frac{2}{C}\{\text{Ln}\,[(\frac{\Theta_0}{\alpha})^2 + 1] - \frac{1}{1 + \alpha^2/\Theta_0^2}\} \qquad 11$$

$$X = \frac{2\text{Ln}(\Theta_0/\alpha)^2 + 2\text{Ln}[\Theta^2/(\Theta^2 + \Theta_0^2)] - C\,\Theta^2/(\Theta^2 + \Theta_0^2)}{2\text{Ln}(\Theta_0/\alpha)^2 - C} \qquad 12$$

We note finally that the inelastic scattering can be neglected in comparison with elastic scattering for elements having a high atomic number and for $\alpha > 2.10^{-2}$ rad. (Table 1).

In the case of silver, for a voltage of 0.5 MV, Figure 2 shows (continuous line) the experimental angular distribution function of electrons transmitted by target of thickness 0.82 μm (Soum et al. 1976). The points represent the results of Monte Carlo calculations with two scattering models: total scattering (relations 4 and 7) or scattering outside an angle $\alpha = 2.10^{-2}$ rad. (relations 8a and 8 b). We note here that the agreement is good whichever way we treat the problem. Moreover, we can use partial cross sections in order to reduce the computing time by a factor of four.

2.3 Energy loss

2.3.1 Energy loss selection While travelling through matter, the electrons suffer inelastic collisions which reduce their incident energy. The superposition of several elementary phenomena makes the theoretical solution of this problem highly complex. Many expressions have been proposed, after much simplification. In Monte Carlo calculations, the choice of energy losses by multiple scattering are deduced from Landau's theory (1944). To find the most probable energy ΔE_p, we express the mean energy loss ΔE_m as follows:

$$\Delta E_m - \Delta E_p = 3.225 \, \xi$$

$$\text{with } \xi = 15.349 \, \frac{\varrho Z}{A} \, \frac{1}{\beta^2} \, s \qquad 13$$

where ξ is expressed in eV, s and ϱ in μm and g/cm³ respectively. Then we have:

$$-\frac{dE}{ds} = \frac{\xi}{\varrho} \left(\text{Ln} \, \frac{\xi}{Q_{min}} - \beta^2 + 3.423 \right) \qquad 14$$

with $Q_{min} = I^2/(2\gamma^2\beta^2 mc^2)$, the minimum energy lost by the primary electron during a collision. Expression (14) may be compared with that of Bethe (1933), which is generally used in Monte Carlo calculations.

An experimental test (Perez, 1975) of these two theories has shown that the mean energy loss given by Bethe (1933) differs still further from the experimental values than that given by the above relation (14). We introduce this mean energy loss when the individual electron step-length Δs_i is such that $\Delta s_i / \Lambda = 10$. We then calculate new values of the cross section until the entire specimen has been traversed. The energy correction is made along the real trajectory of the electrons.

2.3.2 Verification In addition to the above experimental verification (Perez, 1975), we have studied how we can find the electron range in matter by making use of Landau's (1944) law. In the case of particle travelling through a solid medium, it is not only useful to know the mean range $r_L(E_0)$ of this particle of incident energy E_0, but also its penetration depth into the medium. The total range is defined as the minimum thickness of the specimen which makes the coefficient of transmission zero. By considering the normalization properties of transmission curves (Soum et al. 1981b), we propose the following relation for the total electron range in the matter:

$$r = \frac{2.39}{\varrho} \, 10^{-8} \, V^2 \, \left(\frac{1 + \gamma' \, V}{1 + 2\gamma' \, V} \right)^4 \qquad 15$$

with: $\gamma' = 0.978.10^{-6}$

The quantities r, ϱ and V are expressed in μm, g/cm³ and volt respectively. Figure 3 shows that the above model and the experimental results for targets of aluminium, silver and gold are in good agreement.

By using Eq. 14 and the scattering laws (10) and (12), in an earlier work, we have simulated the electron trajectories in a semi-infinite medium. We note that the simulations predict the total range to a good approximation. Thus, in the domain of multiple scattering, we have chosen Landau's (1944) law to represent the rate of loss of energy of the incident beam.

It is now easy to compare the total experimental electron range $r(E_0)$ and the mean theoretical range $r_L(E_0)$, obtained by numerical integration of Eq. 14. In Figure 4, we represent the ratio $r_L(E_0)/r(E_0)$ as a function of E_0 in the case of aluminium and gold; this value is practically independent of the incident energy when $E_0 > 300$ keV.

As already noted (Verdier and Arnal, 1969a), we must distinguish the mean range and the total range except for low atomic number elements higher than aluminium.

2.4 Distribution of step lengths

The laws describing the angular deflection are directly related to the differential cross-sections; the lengths of the steps between successive events will be intimately connected with the mean free paths which are written:

$$\Lambda_\alpha^{-1} = \Lambda_{e\alpha}^{-1} + \Lambda_{i\alpha}^{-1} \qquad 16$$

We cut up the real trajectory of the electron into elements of length Δs, much smaller than the mean free path. A random number X which defines the type of interaction is associated with each of these paths. If an interaction does occur, we calculate the new direction of the electron trajectory by generating a second random number. So we determine the new electron parameters of position and the depth x, until the electron leaves the sample. As we are interested in the backscattering phenomena, we allowed the electron to penetrate into the specimen to a depth of only 0.75 $r(E_0)$ to avoid useless calculation.

The accuracy of the Monte Carlo method depends on the random numbers generated by the computer and on the numbers N of electrons. We carry out our calculation with N = 10,000 incident electrons and with a step length of about $\Lambda_\alpha/4$.

3. RESULTS

3.1 The backscattering coefficient

For a sample of uniform thickness x, the backscattering coefficient is usually defined as the ratio of the number of backscattered electrons to the number of incident electrons. Many theoretical models or semi-empirical expressions have been developed by various authors (Archard, 1961; Everhart, 1960; Frank, 1959; Kanter, 1955; Niedrig, 1977, 1978; Tabata
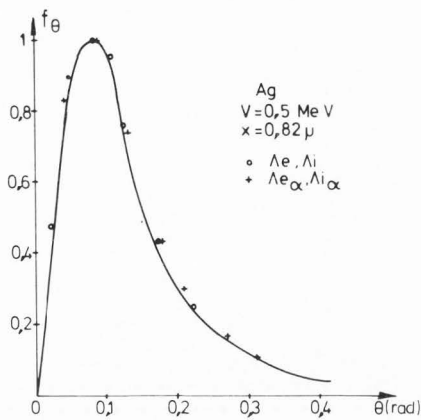
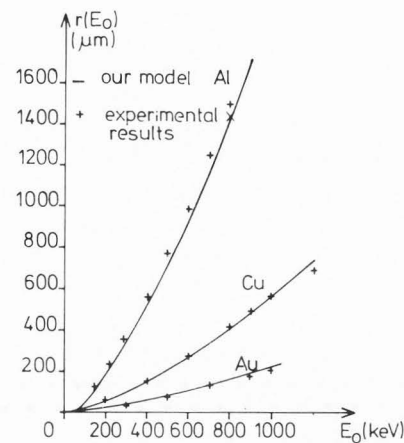**Fig. 2. Angular distribution; scattering models.**
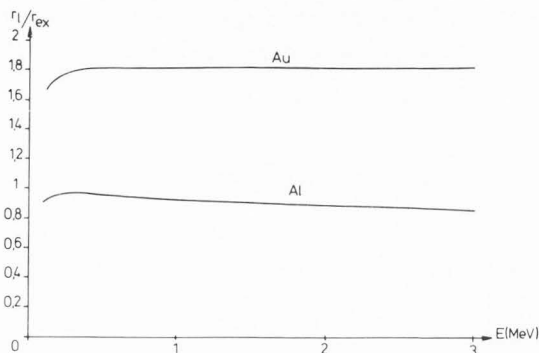

Fig. 3. Variation of electron range.

Fig. 4. Total experimental electron range $r(E_0)$ and the mean theoretical range $r_L(E_0)$ as a function of the energy.
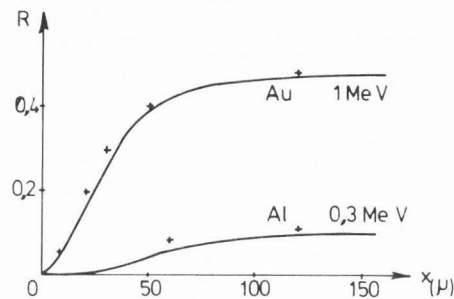

Fig. 5. Backscattering coefficient as a function of the thickness.

Fig. 7. Variation of the backscattering coefficient as a function of the energy for gold targets of various thickness.
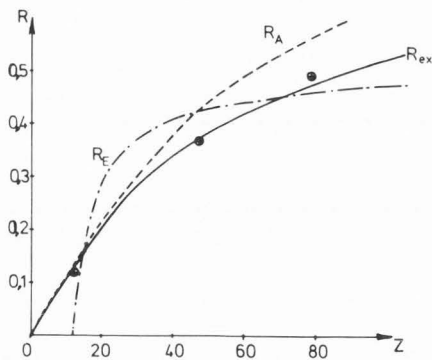

Fig. 6. Variation of the backscattering coefficient as a function of the atomic number.

et al. 1971; Verdier and Arnal, 1969b) for the backscattering coefficient R; but these expressions are satisfactory only at low voltage and for a small range of incident energy E_0. We present here the results of our Monte Carlo calculation for energies ranging from 0.3 to 3 MeV and we compare these results with our experimental measurements and with experimental results of different authors (Tabata et al. 1971).

Experiment shows that, for a given energy of incident electrons, the backscattering coefficient stops increasing beyond a certain thickness x_r. A sample with a thickness greater than or equal to x_r is said to be thick for the energy in question; if
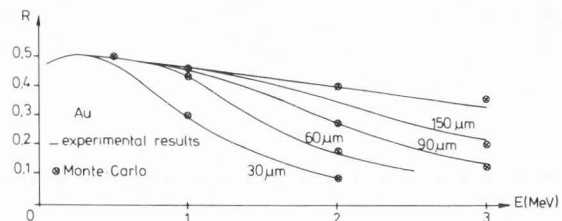
the thickness is less than x_r, it is said to be thin.

Figure 5 shows the variation of R with the thickness of the sample. We have plotted the experimental curves (Verdier and Arnal, 1969b) corresponding to aluminium (0.3 MeV) and to gold (1 MeV); the points were obtained by simulation and the agreement is good.

An experimental study (Verdier and Arnal, 1969b) of the backscattering coefficient for thick samples shows that, for all elements, R does not change very much when the incident energy increases from 0.3 to 1.2 MeV. In this energy range, Figure 6 shows the variation of R for thick samples as a function of atomic number: the experimental results are compared with Everhart's theory (1960) (R_E) and with Archard's model (1961) (R_A); the results of our Monte Carlo calculation fall on the experimental curve.

It is also interesting for a given element, for example gold in Figure 7, to follow the increase of the backscattering coefficient as a function of the energy E_0. We note that the points
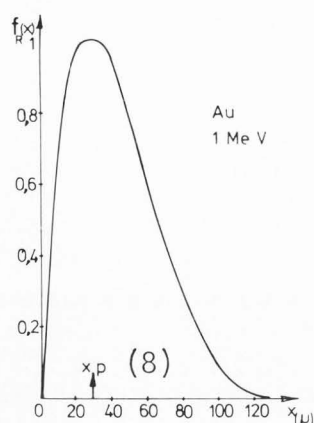
Fig. 8. Depth distribution of the backscattered electrons.

Fig. 9. Normalized angular distribution of backscattered electrons in aluminium for various thickness.

   a) $F_R(\Theta,x)$ is the fraction of backscattered electrons per unit solid angle.

   (b) $f_R(\Theta,x)$ is the function of angular distribution.

corresponding to our calculation are in agreement with the measurements over a wide range of energy, from 0.3 to 3 MeV. Our calculation correctly predicts that R decreases as the energy E_0 increases and that R varies for thin samples.

The method of representation of R in Figure 7 is more suitable than that of Figure 5 for measuring the thickness x_r and the energy E_0 below which the sample is thick. From Figure 3, it is easy to show that $x_r(E_0) \cong r(E_0)/2$, which confirms the suggestion made by certain authors.

For each backscattered electron, it is of interest to know the depth at which it begins to return to the entry surface of the sample. Figure 8 represents the distribution function $f_R(x)$ of the backscattered electrons for a semi-infinite gold target and for an incident electron energy of 1 MeV. We find again that the incident electrons cannot be scattered from beyond a certain depth approximately equal to $r(E_0)/2$, which also justifies the notion of thin and thick targets.

3.2 Angular distribution of backscattered electrons

The angular distribution of backscattered electrons as a function of sample thickness has been studied experimentally by Frank (1959). The function $F_R(\Theta,x)$ defined as the fraction of backscattered electrons per unit solid angle that make an angle Θ with the incident electron direction and the expression $f_R(\Theta,x) = 2\pi \sin \Theta \cdot F_R(\Theta,x)$ is the function of angular distribution of backscattered electrons.

Integration of this function from $\pi/2$ to π gives the corresponding backscattering coefficient. Finally, the angle at which this function passes through a maximum is called the most probable angle of backscattering.

In Figure 9, for example, we represent the normalized angular distribution of backscattered electrons in aluminium for various thicknesses. We see that the function $F_R(\Theta,x)$ becomes narrower as we increase the thickness and, for a given target element, the shape of the angular distribution does not alter beyond a certain thickness of the target equal to one half of the total range of electrons. These results also show that the most probable angle of backscattering increases for a given energy as the thickness of the target increases and then takes a limiting value equal to 140° as we reach the thick sample range.
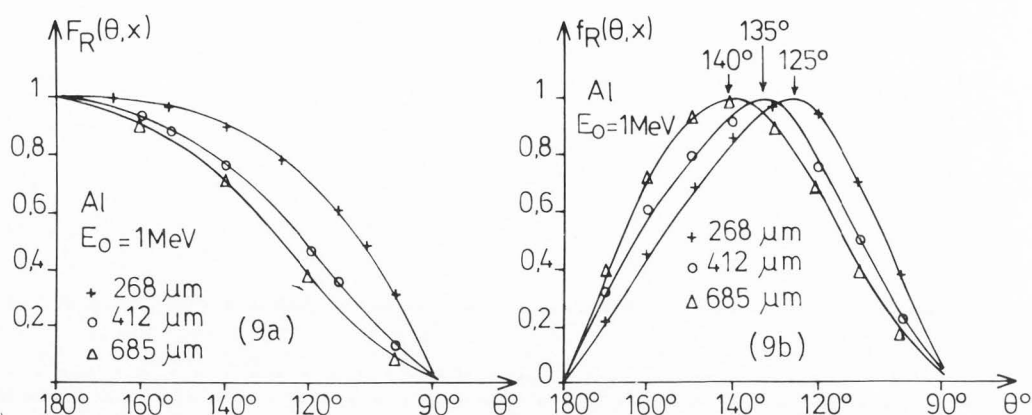
In Figure 10 and Figure 11, the continuous curves represent Frank's (1959) results for thick samples of lead and aluminium respectively. We include the values of our calculation for thickness of aluminium and gold greater than half the total range corresponding to an incident electron energy of 1 MeV. Our study is in agreement with the experimental results of Frank (1959) and reveals a certain deviation relative to the cos Θ law; this deviation becomes large for higher atomic numbers.

3.3 Energy distribution of backscattered electrons

Many authors (Bothe, 1949; Darlington, 1975; Kulenkampff and Spyra, 1954; Matsukawa et al. 1974; Sternglass, 1954; Thümmel, 1964) have experimentally determined for low voltage the energy spectra of the backscattered electrons for the case of thick samples and have also studied the variation of backscattering with the backscattering angle. As an example, we give in Figure 12 the results of our calculation for the energy distribution for an incident electron energy of 1 MeV, backscattered from thick targets of aluminium and gold. We compare these results with the measurements of different authors unfortunately at incident electron energy lower than ours.

It is important to note that the normalized energy distribution function $f(E/E_0)$ is not very sensitive to variations of E_0. Some difference appears at low values of E_0, that is to say for electrons which have lost a large fraction of their incident energy.

However, the most probable energy E_p of backscattered electrons is a characteristic of the element; for gold: $E_p = 0.95\,E_0$ and for aluminium: $E_p = 0.67\,E_0$ in agreement with experimental results. For the average energy of backscattered electrons, we obtain: $E_m = 0.82\,E_0$ for gold samples and $E_m = 0.6\,E_0$ for aluminium samples; the last values are much larger than those given by Sternglass (1954):

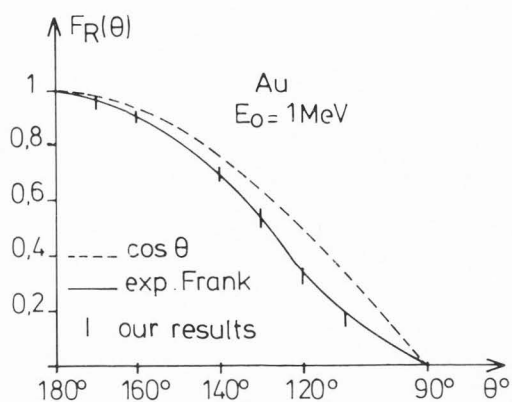$$E_m = (0.45 + 2.10^{-3}\,Z)E_0 \qquad 17$$

Fig. 10. Angular distribution of the backscattered electrons in the case of solid samples of gold.

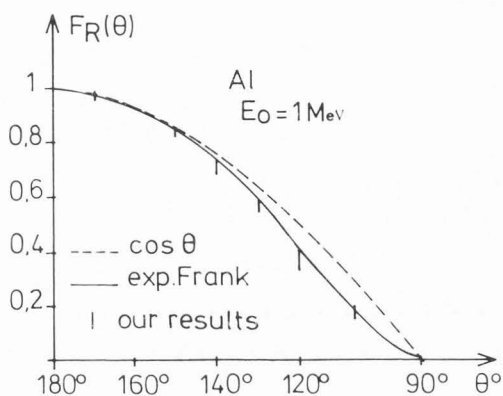(Frank's (1959) experimental curve: continuous line; our results: vertical dash).

Fig. 11. Angular distribution of the backscattered electrons in the case of solid samples of aluminium.

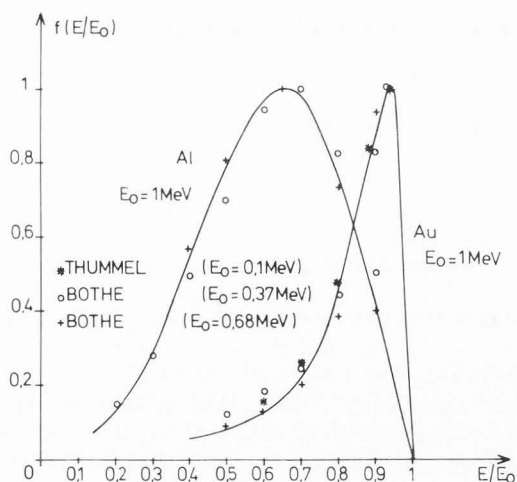(Frank's (1959) experimental curve: continuous line; our results: vertical dash).

Fig. 12. Energy distribution of backscattered electrons ($\bigcirc$ + : Bothe (1949); *: Thümmel (1964).)

This difference is due to the fact that the coefficients in this expression were obtained using low energy incident electrons; this observation is also in agreement with above remark concerning electrons that have lost a large fraction of their incident energy.

4. CONCLUSION

The proposed model of calculation for the study of the backscattered electrons from polycrystalline samples has allowed us to obtain values of the backscattering coefficients in good agreement with the experimental values. These prove the validity of the expression for the cross section and the energy loss which are used.

So far as the analysis of the backscattered electron energy is concerned, our calculation, which corresponds to high energy, allows us to predict the published results for low incident electron energy.

REFERENCES

Archard CD. (1961). Backscattering of electron. J. App. Phys. **32**, 1505-1509.

Arnal F, Balladore JL, Soum G, Verdier P. (1977). Calculation of the cross sections of electron interaction with matter. Ultramicroscopy **2**, 304-310.

Bennett AJ, Roth LM. (1972). Effect of primary electron diffusion on secondary electron emission. Phys. Rev. B. 5, **11**, 4309-4324.

Berger HJ. (1963). Methods in computational physics. Acad. Press, N.Y., **1**, 135-153.

Berger HJ, Seltzer SM. (1964). Mean energy loss of electrons in solids, N. Ac. Sci. Nat. Res. Council Publi. **1133**, 205-218.

Bethe H. (1933). Theory of collisions. Handbuch der Physik. **24**, 491-523.

Bethe H, Rose ME, Smith LP. (1938). The multiple scattering of electrons. Proc. Am. Phil. Soc. **78**, **4**, 573-585.

Bishop HE. (1967). Electron scattering in thick targets. Brit. J. Appl. Phys. **18**, 703-715.

Bothe W. (1949). Einige einfache Uberlegungen zur Rüchdiffusion schneller Elektronen. (About the backscattering of fast electrons.) Annalen der Phys. **6**, 44-52.

Brown DB, Ogilvie RE. (1966). An electron transport model for the prediction of X-rays production and electron backscattering in electron microanalysis. J. Appl. Phys. **37**, 4429-4435.

Brown DB, Wittry DB, Kyser DF. (1969). Prediction of X-rays production and electron scattering in electron — Probe analysis using transport equation. J. Appl. Phys. **40**, 1627-1636.

Darlington EH. (1975). Backscattering of 10-100 keV electrons from thick targets. J. Phys. D: Appl. Phys. **8**, 85-93.

Everhart TE. (1960). Simple theory concerning the reflection of electrons from solids. J. Appl. Phys. **31**, 1483-1490.

Fathers DJ, Rez P. (1979). A transport equation theory of electron backscattering, Scanning Electron Microsc. 1979; I: 55-66.

Frank H. (1959). Zur Vielfachstreuung und Rückdiffusion schneller Elektronen nach Durchgang durch dicke Schichten. (About the multiple scattering and backscattering of fast electrons in thick samples.) Z. Naturforsch. **14**, 247-261.

Henoc J. (1976). Introduction à l'analyse des échantillons minces. (Introduction to the analysis of thin samples.) J. Micr. Spectr. Elect. **1**, 63-71.

Kanter H. (1955). Backscattering of kilovolt electrons from thin films. Brit. J. Appl. Phys. **15**, 555-559.

Kulenkampff H, Spyra W. (1954). Energieverteilung rückdiffundierter Elektronen. (Energy distribution of backscattered electrons.) Z. für Phys. **137**, 416-425.

Landau L. (1944). On the energy loss of fast-particles by ionization. J. of Phys. **8**, 4, 201-205.

Lanteri H, Bindi R, Rostaing P. (1980). Modèle théorique de la rétrodiffusion de'électrons par des cibles massives d'aluminium, d'argent et de cuivre. (Theoretical model of the electrons backscattered from solid targets of aluminium, silver and copper.) J. Phys. D.: Appl. Phys. **13**, 677-692.

Lenz F. (1954). Zur Streuung mittelschneller Elektronen in kleinste Winkel. (Scattering of nearly fast electrons.) Z. Naturforsch. **9a**, 185-204.

Martinez JP. (1978). Contraste des images d'objets amorphes en microscopie électronique à haute tension. (Image contrast of amorphous samples in high voltage electron microscopy.) Thése d'Etat. **812**. University P. Sabatier — Toulouse — French.

Martinez JP, Balladore JL. (1979). Diffusion d'électrons de haute énergie (1.2 à 3 MeV). (Electron diffusion of high energy (1, 2 to 3 MeV.) J. Micr. Spect. Elect. **4**, 1-18.

Matsukawa T, Murata K, Shimizu R. (1973). Investigation of electron penetration and X-rays production in solid targets. Phys. Stat. Sol. **55**, 371-383.

Matsukawa T, Shimizu R, Hashimoto H. (1974). Measurements of the energy distribution of backscattered kilovolt electrons with a spherical retarding field energy analyser. J. Phys. D.: Appl. Phys. **7**, 695-702.

Murata K. (1974). Spatial distribution of backscattering in the scanning electron microscope and electron microprobe. J. Appl. Phys. **45**, 9, 4110-4117.

Niedrig H. (1977). Film thickness determination in electron microscope: the electron backscattering method. Optica Acta. **24**, 6, 679-691.

Niedrig H. (1978). Physical background of electron backscattering. Scanning. **1**, 17-34.

Perez JPh. (1975). Pertes d'énergie en microscopie électronique à trés haute tension. (Energy loss in high voltage electron microscopy.) Thése d'Etat. **723**, University P. Sabatier — Toulouse — French.

Perez JPh. Sevely J, Jouffrey B. (1977). Straggling of fast electron in aluminium foils observed in high-voltage electron microscopy. Phys. Rev. A. **16**, 3, 1061-1069.

Reimer L, Gilde H, Sommer KH. (1970). Die Verbreiterung eines Elektronenstrahles (17-1200 keV) durch Mehrfachstreuung. (Spreading of electron beam by multiple scattering.) Optik. **30**, 590-605.

Shimizu R, Murata K. (1971). Monte Carlo calculations of the electron sample interactions in the scanning electron microscope. J. Appl. Phys. **12**, 1, 387-394.

Soum G, Arnal F, Marais B, Verdier P. (1976). Normalisation des courbes de répartition angulaire des électrons transmis par des feuilles minces de matiére. (Normalization of angular distribution curves of electrons transmitted by thin films of matter.) C.R. Acad. Sci. Paris, **283**, 205-208.

Soum G, Arnal F, Balladore JL, Jouffrey B. (1979). Monte Carlo calculations on electron multiple scattering in amorphous or polycrystalline targets. Ultramicroscopy **4**, 451-465.

Soum G, Ahmed H, Arnal F, Jouffrey B, Verdier P. (1961a). Etude de la rétrodiffusion d'électrons rapides par des échantillons polycristallins. (Study of fast electrons backscattered from polycrystalline sample.) J. Micr. Spect. Elec. **6**, 107-118.

Soum G, Ahmed H, Arnal F, Jouffrey B, Verdier P. (1981b). Le parcours entier des électrons dans la matiére. (The total electron range in the matter.) C.R. Acad. Sci. Paris. **293**, 115-118.

Sternglass EJ. (1954). Backscattering of kilovolt electrons from solids. Phys. Rev. **95**, 2, 345-357.

Tabata T, Ito R, Okabe S. (1971). An empirical equation for the backscattering coefficient of electrons. Nucl. Inst. and Methods. **94**, 509-513.

Thümmel HW. (1964). On the energy distribution of backscattered electrons as a function of deflection angle. Z. fur Phys. **179**, 116-122.

Verdier P, Arnal F. (1969a). Parcours des électrons dans la matiére. (The electron path in matter.) C.R. Acad. Sci., Paris, **268**, 885-888.

Verdier P, Arnal F. (1969b). Calcul du coefficient de rétrodiffusion dans le cas d'électrons monocinétiques. (Calculation of the backscattering coefficient in the case of monokinetic electrons.) C.R. Acad. Sci., Paris, **268**, 1101-1104.

DISCUSSION WITH L. REIMER

Question 1: You obviously obtained Equation 14 from Landau theory. What is the difference to the Bethe formula for continuous slowing down approximation?

Answer: Our Monte Carlo calculation needs an expression for the stopping power ($-dE/ds$). This expresssion is given by the Bethe energy losses law or by Landau theory which gives the most probable energy loss

$$\Delta E_p = \xi \left[\text{Log} \frac{\xi}{Q_{min}} - \beta^2 + 0.198 \right].$$

Since $\Delta E_m - \Delta E_p = 3.225\ \xi$, Landau theory leads to the expression (14) of the stopping power.

In the studied energy ranges, it has been experimentally checked that the expression gives a better experimental result reduction than the Bethe's one.

Question 2: For the calculation of displacement cross-sections from knock-on collisions many authors use Mott scattering cross-sections, i.e. those of McKinley-Feshbach. Have you tried to incorporate these differences to Rutherford cross-sections in your Monte Carlo program?

Answer: Our Monte Carlo calculation is based on the use of the partial cross-sections which indicate the scattering outside an angle α $(10^{-2} \rightarrow 5.10^{-2}\ \text{rad})$. This allows us to neglect the inelastic scattering of electrons. We have not used the Mott or McKinley-Feshbach cross-sections, because we have verified that our cross-sections are in a good agreement with the experimental results.

Question 3: Are the coefficients C and a in (2) obtained by fitting experiments of small angle scattering or can they be got by calculation?

Answer: The parameter a is related to the screening radius of the Wentzel-Yukawa potential. Lenz's theory is valid in the isolated atom model, so we have corrected the calculations by introducing another parameter b which permits to take into account the effect of neighbouring atoms to the scattering center. The potential takes the form:

$$V = \frac{Ze}{r}\ \exp - \left(\frac{r - b}{a}\right)$$

This is equivalent to assign to the nucleus of the atom a charge Ze exp b/a. The parameters a and b have been determined from the experimental results corresponding to the scattering cross-sections.